Published OnlineFirst October 31, 2013; DOI: 10.1158/0008-5472.CAN-13-0436

Molecular and Cellular Pathobiology

Cancer Research

HTLV-1 bZIP Factor Suppresses Apoptosis by Attenuating the Function of FoxO3a and Altering Its Localization

Azusa Tanaka-Nakanishi, Jun-ichirou Yasunaga, Ken Takai, and Masao Matsuoka

Abstract

As the infectious agent causing human adult T-cell leukemia (ATL), the human T-cell leukemia virus type 1 (HTLV-1) virus spreads *in vivo* primarily by cell-to-cell transmission. However, the factors that determine its transmission efficiency are not fully understood. The viral genome encodes the HTLV-1 bZIP factor (HBZ), which is expressed in all ATL cases and is known to promote T-cell proliferation. In this study, we investigated the hypothesis that HBZ also influences the survival of T cells. Through analyzing the transcriptional profile of HBZ-expressing cells, we learned that HBZ suppressed transcription of the proapoptotic gene *Bim* (*Bcl2l11*) and that HBZ-expressing cells were resistant to activation-induced apoptosis. Mechanistic investigations into how HBZ suppresses *Bim* expression revealed that HBZ perturbs the localization and function of FoxO3a, a critical transcriptional activator of the genes encoding Bim and also Fas ligand (FasL). By interacting with FoxO3a, HBZ not only attenuated DNA binding by FoxO3a but also sequestered the inactive form of FoxO3a in the nucleus. In a similar manner, HBZ also inhibited *FasL* transcription induced by T-cell activation. Further study of ATL cells identified other Bim perturbations by HBZ, including at the level of epigenetic alteration, histone modification in the promoter region of the Bim gene. Collectively, our results indicated that HBZ impairs transcription of the *Bim* and *FasL* genes by disrupting FoxO3a function, broadening understanding of how HBZ acts to promote proliferation of HTLV-1–infected T cells by blocking their apoptosis. *Cancer Res; 74(1); 188–200. ©2013 AACR.*

Introduction

Human T-cell leukemia virus type 1 (HTLV-1) is estimated to infect 10 to 20 million people in the world (1). This virus causes not only a neoplastic disease of $CD4^+$ T cells, adult T-cell leukemia (ATL), but also chronic inflammatory diseases of the central nervous system, lung, or skin (2). HTLV-1 can be transmitted efficiently in a cell-to-cell fashion (3, 4), whereas free virus shows poor infectivity (5, 6), and virions are not detected in infected individuals. To increase the number of infected cells and facilitate transmission, HTLV-1 increases its copy number primarily by triggering the proliferation of infected cells, replicating within the host genome instead of undergoing viral replication (7, 8). Thus, HTLV-1 promotes proliferation and suppresses apoptosis of infected cells via complex interactions of viral proteins with host factors.

Among the viral genes encoded in HTLV-1, the *tax* gene has been extensively studied. Tax can activate various signal pathways like NF-κB, AP-1, and SRF (9). However, Tax expression is frequently undetectable in ATL cases. Importantly, the nonsense mutations in the *tax* gene are often observed in not only ATL cases but also infected cells of asymptomatic HTLV-1 carriers (10). These findings suggest that other mechanisms suppress the apoptosis of HTLV-1–infected cells in the absence of Tax expression (2). We have reported that the *HTLV-1 bZIP factor (HBZ)* gene is expressed in all ATL cases (11). Furthermore, HBZ promotes the proliferation of T cells and induces development of T-cell lymphomas and inflammatory diseases in transgenic mice (12). Therefore, we speculated that HBZ might also influence apoptosis.

There are two major pathways for apoptosis: the extrinsic and intrinsic apoptotic pathways, which are mediated by Fas and Bim, respectively (13). ATL cells are known to express high levels of Fas antigen, and are susceptible to Fas-mediated signaling (14). However, FasL expression is suppressed in ATL cells by silencing of the *early growth response 3* (*EGR3*) gene transcription, a phenomenon that enables ATL cells to escape activation-induced cell death (15). In addition, Tax increases expression of c-FLIP, which confers resistance to Fas-mediated apoptosis (16, 17). Furthermore, activation of NF-κB by Tax also enables HTLV-1–infected cells to be resistant to apoptosis (18). To date, the effects of HTLV-1 infection on Bim-mediated apoptosis remain unknown.

In this study, we analyzed transcriptional changes induced by HBZ expression in T cells, and found that transcription of a proapoptotic gene, *Bim*, was hindered by HBZ. This suppression led to decreased activation-induced cell death. We found that HBZ suppressed *Bim* transcription by targeting FoxO3a, a critical transcription factor for the *Bim* and *FasL* gene. In some

Authors' Affiliation: Laboratory of Virus Control, Institute for Virus Research, Kyoto University, Sakyo-ku, Kyoto, Japan

Note: Supplementary data for this article are available at Cancer Research Online (http://cancerres.aacrjournals.org/).

Corresponding Author: M. Matsuoka, Institute for Virus Research, Kyoto University, 53 Shogoin Kawahara-cho, Sakyo-ku, Kyoto 606-8507, Japan. Phone: 81-757-514-048; Fax: 81-757-514-049; E-mail: mmatsuok@virus.kyoto-u.ac.jp

doi: 10.1158/0008-5472.CAN-13-0436

Published OnlineFirst October 31, 2013; DOI: 10.1158/0008-5472.CAN-13-0436

ATL cell lines and ATL cases, the *Bim* gene transcription was also silenced by epigenetic mechanisms, but this phenomenon seemed to be secondary to HBZ-mediated suppression of transcription. Thus, it is suggested that HBZ suppresses both intrinsic and extrinsic apoptotic pathways and contributes to the proliferation of ATL cells.

Materials and Methods

Cell lines and clinical samples

HTLV-1 immortalized cell lines (MT-4), ATL cell lines (ED, TL-Om1, and MT-1), T-cell lines not infected with HTLV-1 (Jurkat, SupT1, and CCRF-CEM) were cultured in RPMI 1640 medium supplemented with 10% FBS and antibiotics at 37°C under a 5% CO_2 atmosphere. Jurkat cells stably expressing spliced form of HBZ (sHBZ), Jurkat-HBZ, were maintained as described previously (19). To construct CCRF-CEM cells stably expressing HBZ, CEM-HBZ, the coding sequence of HBZ was subcloned into pME18Sneo vector and then the expression vector or its empty vector were transfected into CCRF-CEM cells by using Neon (Invitrogen) according to the manufacturer's instructions. Stable transfectants were selected in G418 (1 mg/mL). 293T cells were cultured in Dulbecco's Modified Eagle Medium supplemented with 10% FBS and antibiotics and when 293FT cells were cultured, 500 μg/mL G418 was added. Fas-blocking antibody was purchased from Alexis.

This study was conducted according to the principles expressed in the Declaration of Helsinki. The study was approved by the Institutional Review Board of Kyoto University (G204). All patients provided written informed consent for the collection of samples and subsequent analysis.

Plasmid constructs

Wild-type form of FoxO3a was generated by PCR amplification using Jurkat cDNA library and constitutively active form of FoxO3a (FoxO3aAAA) was also generated by PCR amplification with mutated primers (20). These PCR fragments were then subcloned into pCMV-Tag2B vector and pIRES-hrGFP-1a (Stratagene). The vectors encoding the myc-His-tagged form of HBZ and its mutants used in this study have been described previously (19, 21). We modified pLKO.1-EGFP vector for delivery of anti-FoxO3 short hairpin RNAs (shRNA) to Jurkat, Jurkat-control, and Jurkat-HBZ. shRNA sequence used was 5′-GCACAACCTGTCCTGCATAG-3′. The 6xDBE-Luc construct that contains six FOXO-binding sites known as DAF-16 binding elements (DBE) was kindly provided by Dr. Furuyama (Kagawa Prefectural University of Health Sciences, Kagawa, Japan) and the backbone of this vector was pGL3-basic (Promega; ref. 22).

Luciferase assay

Jurkat cells were transfected with 0.2 μg/well of luciferase reporter plasmid, 1 ng/well of *Renilla* luciferase control vector (phRL-TK), 0.2 μg/well of FoxO3aAAA expression plasmid or its empty vector, and 0.6 μg/well of HBZ expression plasmid or its empty vector with caspase inhibitor Z-VAD-FMK (MBL). Plasmids were transfected using Neon (Invitrogen) according to the manufacturer's instructions. After 24 hours, cells were collected and luciferase activities were measured using the Dual-Luciferase Reporter Assay (Promega). Relative luciferase activity was calculated as the ratio of firefly to *Renilla* luciferase activity. Three independent experiments, each with triplicate transfections, were performed and typical results are shown.

Microarray analysis

Jurkat-control and Jurkat-HBZ were stimulated with phorbol myristate acetate (PMA; 50 ng/mL) and ionomycin (Io; 1 μg/mL) for 9 hours. After the stimulation, cells were collected and total RNA was isolated using TRIzol Reagent (Invitrogen) according to the manufacturer's instructions. We then digested DNA using deoxyribonuclease I (Invitrogen) and cleaned up RNA using RNeasy Mini Kit (Qiagen) according to the manufacturer's instructions. We then synthesized cDNA and performed microarray processing according to the GeneChip Expression Analysis Technical Manual (Affymetrix). All data were analyzed by using GeneSpring GX (Agilent Technologies). The microarray data related to this article have been submitted to the Gene Expression Omnibus under the accession number GSE48029.

Immunofluorescence analysis

293FT cells were transfected with expression vectors using Lipofectamine LTX (Invitrogen) or TransIT (TaKaRa). Twenty-four hours after transfection, cells were reseeded on the poly-L-lysine–coated glass (Matsunami Glass Ind., Ltd.) or poly-D-lysine (Sigma)–coated glass. Twenty-four hours after the reseeding, cells were fixed with 4% paraformaldehyde for 15 minutes and permeabilized with 0.2% Triton X-100 for 15 minutes, and blocked by incubation in 5% BSA/PBS for 30 minutes. For immunostaining, the cells were incubated with anti-Foxo3a, anti-p-Foxo3a (Cell Signaling Technology), Cy3-conjugated anti-c-Myc (Sigma) or biotinylated anti-FLAG (Sigma) antibodies for 1 hour or in case of observation of endogenous expression, cells were incubated overnight at 4°C. Primary antibodies were visualized by incubating the cells with Alexa-Fluor 488–conjugated goat anti-rabbit immunoglobulin G (IgG) antibody (Invitrogen) or AlexaFluor 488–conjugated streptavidin (Invitrogen). Nuclei were stained and mounted with ProLong Gold antifade reagent with 4′,6-diamidino-2-phenylindole (DAPI; Invitrogen). To concentrate nonadherent cells onto a microscope slide, CytoFuge (StatSpin) was used. Fixation and blocking were performed as described earlier.

Assessment of apoptosis

Apoptotic cells were routinely identified by Annexin V-APC (eBioscience) or phycoerythrin (PE) or fluorescein isothiocyanate (FITC; BioVision) -staining according to the manufacturer's instructions and analyzed with a flow cytometer (BD FACSCanto II; BD Biosciences). Data files were analyzed by using FlowJo software (TreeStar).

Real-time PCR

Total RNA was isolated for the analysis using TRIzol reagent. RNA was treated with DNase I to eliminate the genomic DNA. Reverse transcription was performed using random primer and SuperScript III Reverse Transcriptase (Invitrogen). $CD25^-$ $CD4^+$ cells from healthy donor were obtained by using human

Published OnlineFirst October 31, 2013; DOI: 10.1158/0008-5472.CAN-13-0436

CD4 T Lymphocyte Enrichment kit (BD Pharmingen). Then, cells were stimulated with PMA/Io for 9 hours, RNA was isolated, and reverse transcription was performed as described earlier. cDNA products were analyzed by real-time PCR using the Taqman Universal PCR Master Mix (PE Applied Biosystems) or FastStart Universal SYBR Green Master (Roche) and Applied Biosystems StepOnePlus Real-Time PCR System according to the manufacturer's instructions. Specific primers and Taqman probes for the *Bim* gene, *FasL* gene, and *GAPDH* internal control gene were purchased from Applied Biosystems. Primer sequences for the *HBZ* gene and *GAPDH* gene used for the evaluation of the knockdown efficiency in MT-1 cells have been described previously (11, 23). Primer sequences for the *HBZ* gene used for another experiment to evaluate the HBZ expression in Jurkat-HBZ, MT-1, TL-Oml, and ED cells were 5′-ATGGCGGCCTCAGGGCTGTT-3′ and 5′-GCGGCTTTCCTCTTCTAAGG-3′. Primer sequences for the *FoxO3a* gene used were 5′-ACAAACGGCTCACTCTGTCCCAG-3′ and 5′-AGCTCTTGCCAGTTCCCTCATTCTG-3′. All amplifications were conducted in triplicates. The relative quantification was calculated according to the method described in Applied Biosystems ABI prism 7700 SDS User Bulletin #2.

Chromatin immunoprecipitation analysis

Chromatin immunoprecipitation (ChIP) assay was performed according to the protocol recommended by Millipore. Cells were fixed with 1% formaldehyde for 10 minutes at room temperature, washed twice with ice-cold PBS, treated with SDS-lysis buffer (1% SDS, 50 mmol/L EDTA, and 200 mmol/L Tris-HCl) for 10 minutes on ice and then sonicated. Thereafter, the DNA/protein complexes were immunoprecipitated with antibodies specific for acetylated-Histone H3, acetylated-Histone H4, dimethylated-Histone H3 (Lys4), RNA polymerase II clone CTD4H8 (Millipore), trimethylated-Histone H3 (Lys27), anti-trimethyl-Histone H3 (Lys9) antibodies (Cell Signaling Technology), or normal rabbit IgG (Santa Cruz Biotechnology) overnight at 4°C. Immune complexes were collected with salmon sperm DNA-protein A and G Sepharose slurry, washed, and eluted with freshly prepared elution buffer (1% SDS, 100 mmol/L $NaHCO_3$). Protein-DNA complexes were de-cross-linked at 65°C for 4 hours. DNA was purified and subjected to real-time PCR for quantification of the target fragments. Sequences for the primer set are described previously (24, 25). For the evaluation of binding of FoxO3a to the FOXO-binding sites, 293T cells were transfected with 5 μg of 6xDBE-Luc construct, 5 μg of FoxO3aAAA expression plasmid together with or without 5 μg of HBZ plasmid using TransIT in 10-cm dishes. Anti-FLAG (Sigma) antibody was used for the immunoprecipitation. Primers used were 5′-AGTGCAGGTGCCAGAACATT-3′ and 5′-GCCTTATGCAGTTGCTCTCC-3′, which were constructed inside of the pGL3-basic vector. For the evaluation of the DNA-binding capacity of FoxO3a with or without HBZ, expression vectors for the HA-tagged FoxO3a and Flag-tagged HBZ were transiently cotransfected into 293T cells using the TransIT reagent. Twenty-four hours after the transfection, cells were collected and chromatin immunoprecipitation assay was performed as described earlier. For the immunoprecipitation, anti-HA (Sigma) antibody was used. Primers used for *Bim* gene promoter were 5′-CCACCACTTGATTCTTGCAG-3′ and 5′-TCCAGCGCTAGTCTTCCTTC-3′, which were constructed to contain the FOXO-binding sequence located in intron1. Primers used for *FasL* gene promoter were 5′-ACGATAGCACCACTGCACTCC-3′ and 5′-GGCTGCAAACCAGTGGAAC-3′, which were also constructed to contain the three FOXO-binding sequences.

Individual PCRs were carried out in triplicate to control for PCR variation and mean C_t values were collected. Fold difference of the antibody-bound fraction (IP) versus a fixed amount of input (In) was calculated as

$$\mathrm{IP/In} = 2^{-\Delta\Delta C_t} = 2^{-(C_t(\mathrm{IP}) - C_t(\mathrm{In}))}$$

Then, the fold difference value for a target antibody (t) was subtracted by the nonspecific value derived from mouse or rabbit IgG (t_0):

$$(\mathrm{IP/In})^t - (\mathrm{IP/In})^{t_0}$$

Bisulfite genomic sequencing

Sodium bisulfite treatment of genomic DNA was performed as described previously (26). DNA regions were amplified using bisulfite-treated genomic DNA by nested PCR. To amplify promoter region (promoter 1) of *Bim*, primers used in the first PCR were 5′-TTTAGAGGGAGGAGAGTTTAAAG-3′ and 5′-CCCTACAACCCAACTCTAACTA-3′. Primers for the second PCR were 5′-AGGGTATAGTGAGAGCGTAGG-3′ and 5′-CAACTCTAACTAACGACCCC-3′. For promoter, two primers used in the first PCR were 5′-GTGTGATTGTTTTTTGAGGG-3′ and 5′-AAAATACCCCCAAACAAAATAC-3′. Primers for the second PCR were 5′-GCGGATTTAGTTGTAGATTTTG-3′ and 5′-ACTCTTTACCCAAAACAAACTTC-3′. PCR products were purified, cloned into pGEM-T Easy vector (Promega), and sequenced using the ABI PRISM 3130 Genetic Analyzer. For CpG methylation analysis, Web-based bisulfite sequencing analysis tool called QUMA (quantification tool for methylation analysis) was used (27).

Coimmunoprecipitation assay, analysis of the p-FoxO3a localization, and immunoblotting

Expression vectors for the relevant genes were transiently cotransfected into 293T cells using the TransIT reagent. Forty-eight hours later, cells were collected and coimmunoprecipitation assays were performed as described previously (28). For the analysis of the p-FoxO3a localization, nuclear and cytoplasmic proteins were extracted using Nuclear Complex Co-IP Kit (Active Motif). The proteins were subjected to SDS-PAGE analysis followed by immunoblotting with various antibodies. Antibodies used were anti-p-FoxO3a, anti-α-tubulin (Sigma), anti-FLAG, anti-HA (Sigma), and anti-His (Marine Biological Laboratory).

Lentiviral vector construction and transfection of the recombinant lentivirus

Lentiviral vector expressing shRNA against HBZ was constructed and recombinant lentivirus was infected as described previously (11). When more than 90% of cells expressed

Published OnlineFirst October 31, 2013; DOI: 10.1158/0008-5472.CAN-13-0436

enhanced green fluorescent protein (EGFP), the *HBZ* and *Bim* gene expressions were analyzed by real-time PCR.

Results

The *Bim* gene transcription is suppressed in HBZ-expressing Jurkat and CCRF-CEM cells

To determine the effects of HBZ on gene expression, we first performed microarray analysis. Jurkat cells with or without expression of spliced form of HBZ (Jurkat-HBZ and Jurkat-control, respectively) were stimulated with PMA and Io for 9 hours. Gene expression profiles were then analyzed by DNA microarray. Table 1 shows the apoptosis-associated genes that were downregulated or upregulated in stimulated Jurkat-HBZ cells. Transcription of the *Bim* gene was prominently downregulated in HBZ-expressing Jurkat cells. To confirm the effect of HBZ on the *Bim* gene expression, we evaluated *Bim* mRNA levels in Jurkat-control and Jurkat-HBZ cells with or without PMA/Io stimulation using real-time PCR. As reported in the previous studies showing that treatment by PMA/Io or other stimulators induced *Bim* expression (29, 30), the *Bim* mRNA level of stimulated Jurkat-control cells was three-times higher than that of unstimulated cells, but that of Jurkat-HBZ cells did not change after stimulation (Fig. 1A). Similarly, increased *Bim* transcription by stimulation was also inhibited by HBZ in CCRF-CEM cells (Fig. 1A).

HBZ inhibits apoptosis

It has been reported that Bim plays an important role in activation-induced cell death and T-cell homeostasis (31). Because the earlier data demonstrated that HBZ inhibits stimulation-induced *Bim* expression, we next investigated whether HBZ inhibits apoptosis in response to PMA/Io stimulation. To test this, Jurkat-control and Jurkat-HBZ were each incubated with or without PMA/Io for 9 hours, and then apoptosis was measured using Annexin V. The percentages of apoptotic cells in Jurkat-control and Jurkat-HBZ were 40.2% and 15% respectively, indicating that HBZ suppressed activation-induced apoptosis (Fig. 1B). We also treated cells with doxorubicin and found that HBZ slightly inhibited doxorubicin-induced apoptosis (Supplementary Fig. S1). Fas-mediated apoptotic pathway might be involved in antiapoptotic effect by HBZ. To assess the effect of Fas-mediated signaling on the activation-induced apoptosis, cells were also treated with or without Fas-blocking antibody (0.5 μg/mL) 30 minutes before the PMA/Io stimulation. The percentage of apoptotic cells without Fas-blocking antibody in Jurkat-control and Jurkat-HBZ were 36.9% and 22.4%, respectively. When cells were treated with Fas-blocking antibody, the percentage of apoptotic cells reduced and those were 24% and 13.2% in Jurkat-control and Jurkat-HBZ, respectively (Fig. 1C). Thus, Fas-blocking antibody partially inhibited apoptosis in Jurkat-HBZ, which indicates that Fas-mediated signals are also implicated in activation-induced cell death. Indeed, we found that the transcription level of *FasL* was suppressed in stimulated Jurkat-HBZ and CEM-HBZ cells compared with Jurkat-control and CEM-control cells (Fig. 1D), suggesting that downregulation of FasL by HBZ was also associated with inhibition of apoptosis.

Table 1. Apoptosis-associated genes that are upregulated or downregulated by HBZ

Gene	Fold change	Gene ontology
API5	2.18	Antiapoptosis
BCL2L11 (Bim)	−9.93	Induction of apoptosis
CARD11	2.87	Regulation of apoptosis
CASP1	2.97	Apoptosis
CD28	4.60	Positive regulation of antiapoptosis
COP1	9.41	Regulation of apoptosis
DEDD2	2.01	Induction of apoptosis via death domain receptors
DYRK2	2.16	Induction of apoptosis
GZMB	−5.90	Apoptosis
HIPK2	2.19	Induction of apoptosis by intracellular signals
NLRP1	3.08	Induction of apoptosis
PI3KR2	−2.68	Negative regulation of antiapoptosis
PLEKHF1	2.99	Induction of apoptosis
PRDX2	−2.10	Antiapoptosis
PRF1	3.95	Virus-infected cell apoptosis
RFFL	2.20	Apoptosis
SPHK1	−4.26	Antiapoptosis
TNFRSF9	−2.61	Induction of apoptosis
TP53INP1	2.32	Apoptosis
VEGFA	−6.96	Negative regulation of apoptosis

NOTE: The table shows a list of apoptosis-associated genes that were downregulated or upregulated (by more than 2-fold) in stimulated Jurkat-HBZ cells identified by microarray analysis.

Published OnlineFirst October 31, 2013; DOI: 10.1158/0008-5472.CAN-13-0436

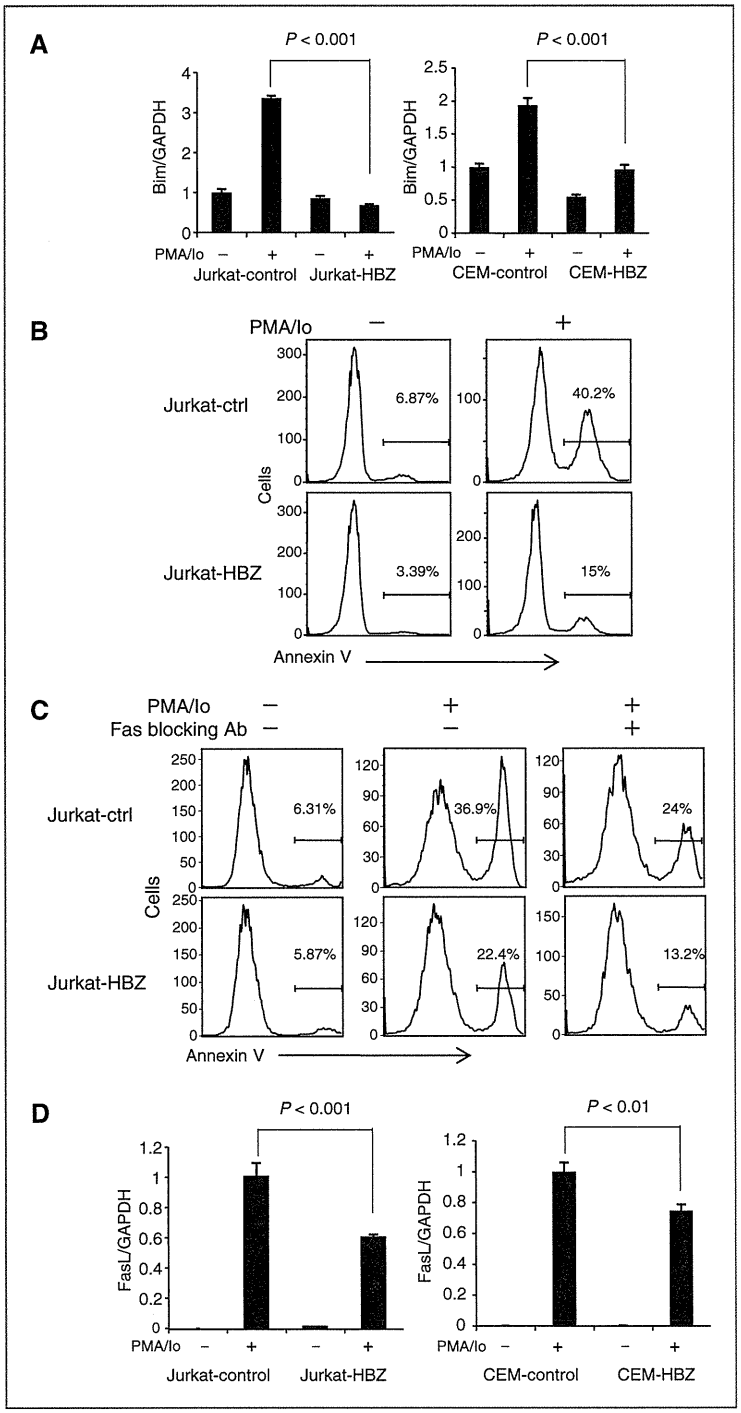

Figure 1. HBZ suppresses the transcription of the *Bim* and *FasL* genes and consequently stimulation-induced apoptosis. A, comparison of the *Bim* mRNA expression in the Jurkat-control, Jurkat-HBZ, CEM-control, and CEM-HBZ cells with or without PMA/Io stimulation by real-time PCR. B, Jurkat-control and Jurkat-HBZ were stimulated with PMA/Io for 9 hours and stained with Annexin V. Percentage of apoptotic cells was determined by flow cytometry. C, Jurkat-control and Jurkat-HBZ were treated with Fas-blocking antibody for 30 minutes and then stimulated with PMA/Io for 9 hours. Percentages of apoptotic cells were monitored by flow cytometry. D, comparison of the *FasL* mRNA transcription in the Jurkat-control, Jurkat-HBZ, CEM-control, and CEM-HBZ cells with or without PMA/Io stimulation by real-time PCR. Error bars, standard deviation. Statistical differences are calculated by Student *t* test. GAPDH, glyceraldehyde-3-phosphate dehydrogenase.

Published OnlineFirst October 31, 2013; DOI: 10.1158/0008-5472.CAN-13-0436

HBZ suppresses *Bim* expression through attenuation of FoxO3a

We analyzed how HBZ suppresses the expression of *Bim* and *FasL*. It has been reported that a forkhead factor, FoxO3a, and p73 are important for the transcription of *Bim* and *FasL* (32, 33). FoxO3a and other FOXO family members are phosphorylated by protein kinases such as Akt or SGK on highly conserved serine and threonine residues (especially Thr32, Ser253, and Ser315 in FoxO3a), resulting in impaired DNA-binding activity and increased binding to the chaperone protein, 14-3-3 (20, 34, 35). Newly formed 14-3-3-FOXO complexes are then exported from the nucleus, thereby inhibiting FOXO-dependent transcription of key target genes such as *Bim*, *FasL*, and *TRAIL* (36).

First, we investigated whether FoxO3a is implicated for the activation induced cell death. As shown in Supplementary Fig. S2, the knockdown of FoxO3a resulted in the decreased apoptotic rate in Jurkat-control cells ($P < 0.05$). Furthermore, inhibition of Foxo3a did not influence activation-induced cell death in Jurkat-HBZ cells, suggesting the inhibitory effect of HBZ on Foxo3a function. To investigate whether HBZ affects FoxO3a function, Jurkat cells were transiently transfected with a plasmid expressing FoxO3aAAA, the constitutive active mutant of FoxO3a, which is no longer phosphorylated by Akt and is localized in the nucleus. The FoxO3aAAA was expressed together with hrGFP using an internal ribosome entry site (IRES; FoxO3aAAA-IREShrGFP). Jurkat cells were transiently transfected with full-length HBZ or its mutants. HBZ has three domains, an activation domain (AD), a central domain (CD), and a basic leucine zipper domain (bZIP; ref. 12). In this study, the deletion mutants (HBZ-ΔAD, HBZ-ΔbZIP, and HBZ-ΔCD) were used. The percentage of FoxO3aAAA induced apoptotic cells in the absence of HBZ was 69.6% while it was suppressed by HBZ (40.6%; $P < 0.001$; Fig. 2A). We also found that an HBZ mutant without activation domain lacks the activity to inhibit FoxO3aAAA-induced apoptosis (Fig. 2A), indicating the significance of activation domain in suppression of FoxO3a-mediated apoptosis. It has been reported that LXXLL motif in FoxO3a binds to its coactivator CBP/p300 (37). Similarly, HBZ has LXXLL-like motifs located in the NH_2-terminal region, which bind to KIX domain of CBP/p300 (38). We speculated that the LXXLL-like motifs of HBZ might affect FoxO3aAAA function through KIX domain of CBP/p300. An HBZ mutant, which has substitutions in 27th and 28th residues (LL to AA) of LXXLL-like motif, lack the activity to suppress FoxO3aAAA-mediated apoptosis (Fig. 2B), indicating that LXXLL-like motif of HBZ is critical for suppression of FoxO3a-mediated apoptosis.

Next, we analyzed the effect of HBZ on a FoxO3a responsive reporter. As shown in Fig. 2C, HBZ suppressed FoxO3a-mediated transcriptional activity ($P < 0.01$). To check whether HBZ inhibits DNA binding of FoxO3a, 293T cells were transiently transfected with FoxO3aAAA and FoxO3a reporter, 6xDBE-Luc, together with or without HBZ. The interaction of FoxO3aAAA to FOXO-binding sites was analyzed by ChIP assay. As shown in Figure 2D, the interaction of FoxO3aAAA to the FOXO-binding sites was interfered by HBZ, suggesting that HBZ inhibits FoxO3a-mediated apoptosis through suppression of the DNA binding of FoxO3a. To clarify the mechanism of HBZ-mediated FoxO3a inhibition, we examined interaction between HBZ and FoxO3a by the immunoprecipitation assay. It showed that HBZ interacted with FoxO3a (Fig. 2E and F). Experiments with FoxO3a deletion mutant revealed that HBZ interacted with the forkhead domain of FoxO3a (Fig. 2E). Analysis using HBZ deletion mutants showed that the central domain of HBZ interacted with FoxO3a (Fig. 2F).

HBZ inhibits nuclear export of phosphorylated form of FoxO3a

Next, we investigated the effect of HBZ on FoxO3a localization by confocal microscopy. We cotransfected 293FT cells with a plasmid expressing human wild-type FoxO3a (FoxO3aWT) protein and an HBZ-expressing plasmid. Consistent with previous reports, FoxO3a remained mainly in cytoplasm when cells were cotransfected with empty vector (Fig. 3A; refs. 20, 34). However, when it was expressed along with HBZ, FoxO3a was localized in both nucleus and cytoplasm (Fig. 3A). To determine whether mislocalized FoxO3a is phosphorylated (pFoxO3a) or not, we used anti-pFoxO3a antibody. Figure 3B and C demonstrated that nuclear-localized FoxO3a was phosphorylated in HBZ-expressing cells. Thereafter, we analyzed the localization of endogenous FoxO3a in HeLa and an ATL cell line, MT-1. Although pFoxO3a was localized widely both in cytoplasm and nucleus in HeLa cells, most pFoxO3a was localized in the nucleus in MT-1 (Fig. 3D), suggesting that endogenous HBZ inhibits the extranuclear translocation of pFoxO3a in this cell line. From the study of crystal structure of the human FoxO3a-DBD/DNA complex, it has been reported that phosphorylation at Ser253 causes a decrease on the DNA-binding ability (39). Abnormal localization of phosphorylated FoxO3a by HBZ might interfere the function of unphosphorylated FoxO3a in the nucleus. The abnormal localization of pFoxO3a prompted us to investigate whether HBZ bound to 14-3-3 along with FoxO3a, as 14-3-3 is a chaperon protein involved in nuclear–cytoplasm shuttling of FOXO family. As shown in Figure 3E, HBZ, FoxO3a, and 14-3-3 form a ternary complex. However, the binding of FoxO3a and 14-3-3 was not affected by HBZ (result of IP with anti-FLAG antibody and detected with anti-HA antibody).

As another possible mechanism for downregulation of *Bim* and *FasL*, we compared the transcription level of *p73* in Jurkat cells with and without HBZ expression. Activation of HBZ-expressing cells reduced transcription of *p73*, but the expression level of *p73* was variable among ATL cell lines (Supplementary Fig. S3A and S3B). We conclude that p73 is not responsible for suppression of *Bim* expression in ATL cells.

Bim expression is suppressed in both ATL cell lines and ATL cases

HBZ has been shown to suppress Bim expression through two different mechanisms as revealed in this study. To analyze Bim expression in ATL cells, we studied *Bim* mRNA levels in non-ATL cell lines and ATL cell lines with or without PMA/Io stimulation, and found that the *Bim* gene transcript was upregulated in Jurkat and CCRF-CEM cells, but not in SupT1 after activation. However, *Bim* transcripts were not increased

Published OnlineFirst October 31, 2013; DOI: 10.1158/0008-5472.CAN-13-0436

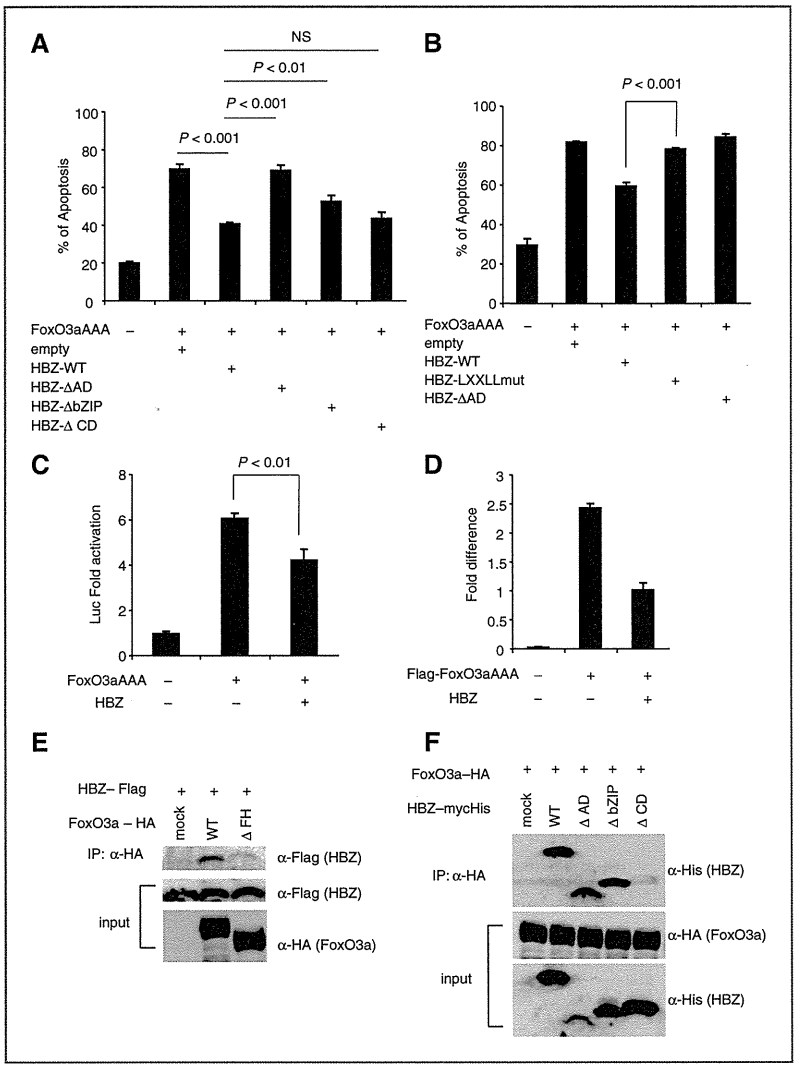

Figure 2. HBZ attenuates function of Foxo3a by physical interaction. A, Jurkat cells were transfected with FoxO3aAAA-expressing vector, a constitutively active form, by using Neon with or without HBZ or its mutants. Twenty-four hours after transfection, cells were stained with Annexin V and analyzed by flow cytometry ($n = 3$). B, Jurkat cells were transfected with FoxO3aAAA-expressing vector together with HBZ or its mutants by using Neon. Cells were stained with Annexin V and analyzed by flow cytometry ($n = 3$). Data are representative of three independent experiments. C, reporter construct containing the 6xDBE and FoxO3aAAA-expressing vector was transiently transfected with or without HBZ into Jurkat cells in the presence of Z-VAD-FMK and luciferase activities were measured. D, 293T cells were transfected with 6xDBE-Luc construct and Flag-tagged FoxO3aAAA expression vector together with or without HBZ expression vector. Cells were immunoprecipitated with anti-FLAG antibody and quantified by real-time PCR. Three independent ChIP experiments were done and representative data are shown. Error bars, experimental variation. E and F, the expression vectors of the indicated proteins were cotransfected into 293T cells, and their interactions were analyzed by immunoprecipitation assay. Data are representative of three independent experiments. Statistical differences are calculated by Student *t* test.

in all stimulated ATL cell lines (Fig. 4A). The *Bim* gene transcript was also downregulated in primary ATL cells (Fig. 4B) compared with resting peripheral blood mononuclear cells (PBMC) and phytohemagglutinin (PHA)-stimulated T cells. We also stimulated primary ATL cells and normal $CD4^+$ T cells with PMA/Io. The *Bim* gene transcription was quite low in primary ATL sample compared with normal $CD4^+$ T cells even though the cells were stimulated with PMA/Io (Fig. 4C). To confirm HBZ expression in representative ATL cell lines, we quantified the level of the *HBZ* mRNA transcription in Jurkat-HBZ, CEM-HBZ, MT-1, ED, and TL-Om1 by real-time PCR and confirmed that HBZ is expressed in these ATL cell lines (Supplementary Fig. S4). Microarray data, obtained from Gene Expression Omnibus (GEO), show that both *Bim* and *FasL* transcription levels are lower in ATL cases than healthy donors (accession number: GSE33615; Supplementary Fig. S5), supporting our data that *Bim* expression was suppressed in ATL cells.

Bim expression is silenced by epigenetic mechanisms

Because the *Bim* gene transcription was severely suppressed in ATL cells, we investigated the epigenetic status (DNA methylation and histone modification) of the promoter region of the *Bim* gene in ATL cells. A previous study showed that the 0.8 kb region immediately upstream of exon 1 contains the important elements for the control of *Bim* expression

Published OnlineFirst October 31, 2013; DOI: 10.1158/0008-5472.CAN-13-0436

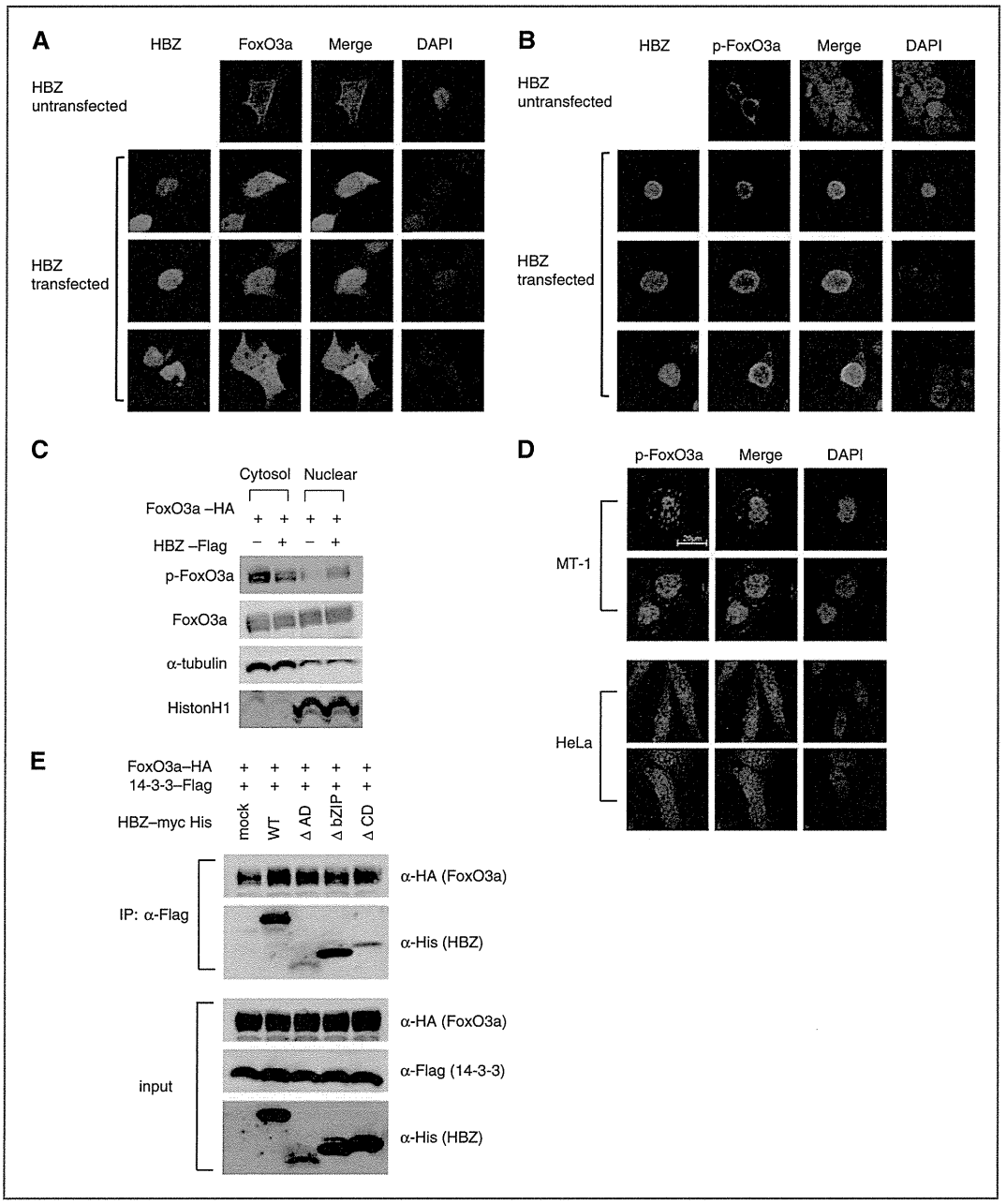

Figure 3. HBZ interferes with normal localization of FoxO3a by forming a ternary complex with FoxO3a and 14-3-3. 293FT cells were transfected with FoxO3aWT-Flag together with or without mycHis-HBZ. A and B, FoxO3a was detected using anti-FLAG-biotin and secondary Streptavidin-Alexa 488 (A), and p-FoxO3a was detected using anti-p-FoxO3a (ser253) and secondary anti-rabbit IgG-Alexa 488 antibody (B). DAPI was used to counterstain the nucleus. C, 293FT cells were transfected with HA-tagged FoxO3aWT together with or without Flag-tagged HBZ. Cytoplasmatic and nuclear fractions were extracted and p-FoxO3a was detected by Western-blotting. D, endogenous localizations of p-FoxO3a (ser253) in HeLa and MT-1 cells were examined using anti-p-FoxO3a. E, the interactions among HBZ, FoxO3a, and 14-3-3 were analyzed by immunoprecipitation.

Published OnlineFirst October 31, 2013; DOI: 10.1158/0008-5472.CAN-13-0436

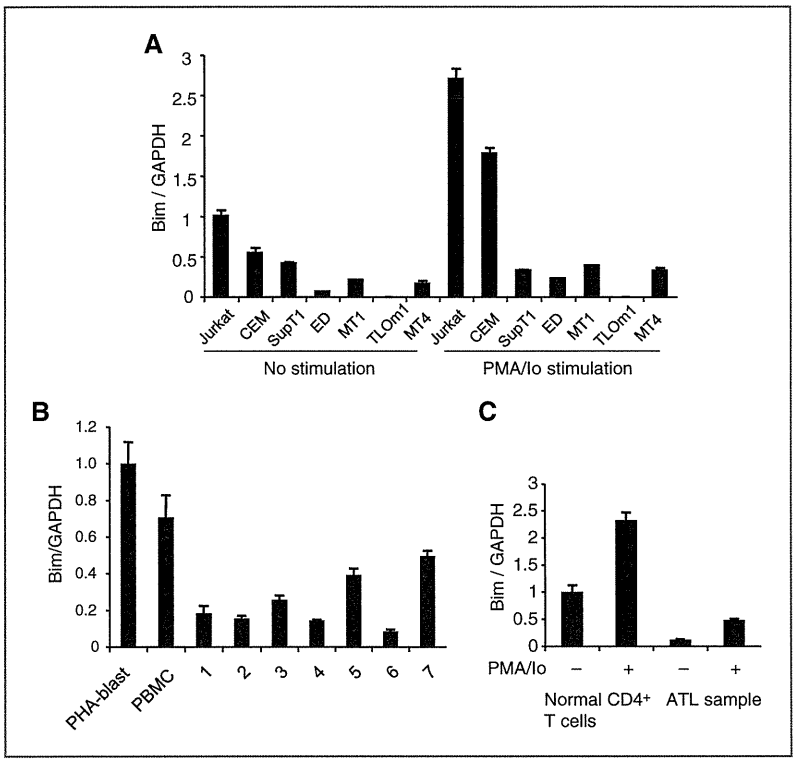

Figure 4. Bim expression is also suppressed in ATL cell lines and ATL cases. Comparison of the *Bim* mRNA expression in non-ATL cell lines and ATL cell lines with or without PMA/Io stimulation (A) and in PBMCs and PHA-blasts from healthy donor samples and fresh ATL samples (B) by real-time PCR. C, comparison of the *Bim* mRNA expression in healthy donor sample and ATL fresh sample with or without PMA/Io stimulation.

(promoter 1). The *Bim* promoter does not contain a TATA or CAAT box and has the characteristics of a "TATA-less" promoter (40). In addition, the alternative promoter has been reported to exist in intron 1 (promoter 2; refs. 41, 42). These two promoter regions are highly GC-rich and contain the binding sites for several transcription factors, including FoxO3a. To determine whether CpG sites in these *Bim* gene promoter regions are methylated in ATL cell lines, their methylation status was analyzed by bisulfite-mediated methylcytosine mapping (Supplementary Fig. S6A and S6B). The promoter 1 of *Bim* was hypermethylated in two ATL cell lines (ED and TL-Om1) and ATL case 1, whereas this region was not so methylated in MT-1 cells and two ATL cases. On the other hand, the promoter 2 was heavily methylated in two ATL cell lines (TL-Om1 and MT-1) and ATL case 1 and partially methylated in Jurkat cells (Supplementary Fig. S6B). These results suggest that in some cases, heavily methylated CpG sites of promoter 1 and 2 are associated with silencing of *Bim* transcription but these methylations can not account for suppressed *Bim* expression in all ATL cell lines and ATL cases.

Therefore, we next focused on the histone modification in the promoter region of *Bim*. It is well known that deacetylation of the histones are also common features of cancer, which results in transcriptional silencing of tumor suppressor genes (43). First, we analyzed the histone H3 and H4 acetylation and H3K4 trimethylation, which are all permissive marks (44), in promoter 1 of Jurkat, MT-1, and TL-Om1 cells. Contrary to our speculation, neither H3, H4 acetylation, nor H3K4 trimethylation differed between MT-1 and Jurkat cells (Supplementary Fig. S7). We next analyzed the histone modification status in promoter 2. As shown in Figure 5A, MT-1 and TL-Om1 cells exhibited decreased level of histone H3 acetylation and H3K4 trimethylation but not histone H4 acetylation. Because methylation of DNA is often preceded by dimethylation of H3K9 or trimethylation of H3K27 (both repressive marks) in oncogenesis (44), we asked whether there were differences in these epigenetic chromatin marks on the *Bim* gene promoter in ATL cell lines. TL-Om1 cells exhibited upregulated level of H3K9 dimethylation and H3K27 trimethylation compared with Jurkat cells (Fig. 5B and C), whereas MT-1 exhibited a little upregulated level of H3K27 trimethylation (Fig. 5C) in the promoter 2. These data suggest that histone modifications of promoter 2 are critical for the suppressed *Bim* gene transcription. We also performed ChIP analysis using anti-RNA polymerase II antibody (Fig. 5D) and revealed that Pol II binding was decreased in MT-1 and TL-Om1 cells, confirming suppressed transcription of the *Bim* gene. To further investigate the mechanisms involved in FoxO3a-mediated *Bim* gene transcription in the promoter 2, we transfected HA-tagged FoxO3a expression vector together with or without a HBZ expression vector into 293T cells and immunoprecipitated with anti-HA antibody. Then, the DNA-binding capacity of FoxO3a was

Published OnlineFirst October 31, 2013; DOI: 10.1158/0008-5472.CAN-13-0436

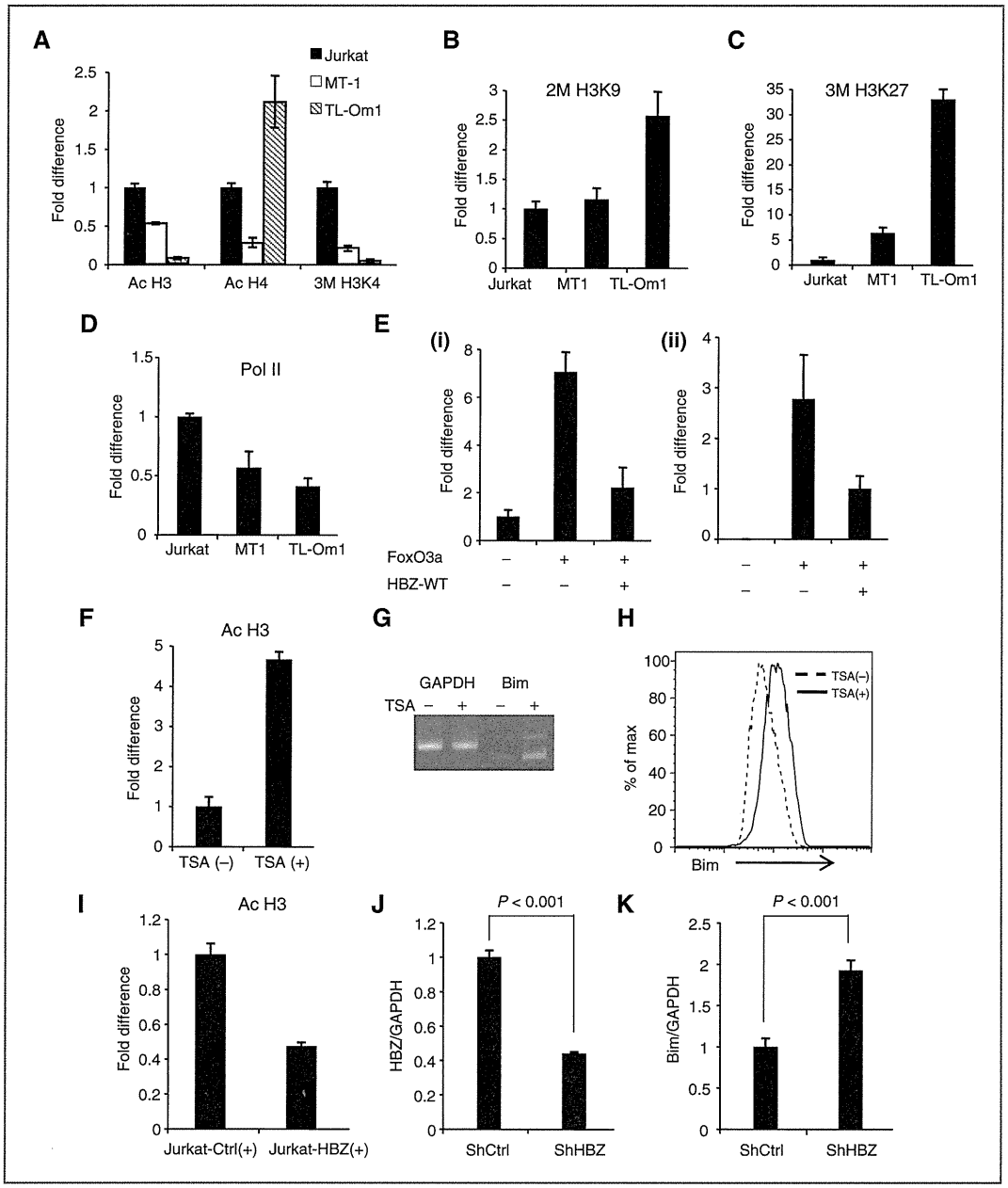

Figure 5. Epigenetic status of the promoter regions of the *Bim* gene. A–C, fold difference of acetylated histone H3, acetylated histone H4, trimethylated H3K4, dimethylated H3K9, or trimethylated H3K27; the data from Jurkat cells were arbitrarily set as 1.0. D, quantitative ChIP assay using RNA polymerase II (Pol II) antibody in Jurkat, MT-1, and TL-Om1 cells. E, 293T cells were transfected with HA-tagged FoxO3a expression vector together with or without HBZ expression vector. Cells were immunoprecipitated with anti-HA antibody and DNA-binding ability at promoter 2 was quantified by real-time PCR. F, fold difference of acetylated histone H3 in MT-1 cells, which were treated with or without 0.4 mmol/L TSA for 15 hours. The data from MT-1 cells without TSA treatment were arbitrarily set as 1.0. G and H, MT-1 cells were treated with 0.4 mmol/L TSA for 15 hours and *Bim* expression level was analyzed by quantitative real-time PCR and flow cytometry. I, fold difference of acetylated histone H3 in the Bim promoter in the Jurkat-control and Jurkat-HBZ cells 9 hours after the stimulation with PMA/Io. J, HBZ transcript in shRNA transfectant of MT-1 was quantified by real-time PCR. K, comparison of the *Bim* mRNA expression in control MT-1 cells and HBZ-KD MT-1 cells. Error bars, experimental variation. The data shown are representative of two or three independent experiments. Statistical differences are calculated by Student *t* test. GAPDH, glyceraldehyde-3-phosphate dehydrogenase.

Published OnlineFirst October 31, 2013; DOI: 10.1158/0008-5472.CAN-13-0436

quantified by real-time PCR. Figure 5E shows that HBZ attenuated the DNA-binding capacity of FoxO3a in the promoter 2 of *Bim* (i) and *FasL* promoter (ii), suggesting that the suppressed binding of FoxO3a to the promoter regions leads to inhibition of the *Bim* and *FasL* genes transcription by HBZ.

Next, we treated MT-1 cells with trichostatin A (TSA), a cell-permeable chemical inhibitor of class I/II histone deacetylases (HDAC). Treatment of TSA resulted in a clear upregulation of acetylation of histone H3 (Fig. 5F) followed by Bim expression both at the mRNA (Fig. 5G) and protein levels (Fig. 5H), indicating that histone modification is associated with suppressed *Bim* transcription in MT-1. We also performed ChIP assay using Jurkat-control and Jurkat-HBZ cells, which were stimulated with PMA and ionomycin for 9 hours, and found that acetylation of histone H3 decreased in Jurkat-HBZ cells (Fig. 5I), suggesting that HBZ is implicated in histone deacetylation in T cells. To verify whether HBZ inhibits transcription of the *Bim* gene, we suppressed the *HBZ* gene transcription by shRNA as reported previously (11). Efficiencies of lentivirus vector transduction, which were determined by EGFP expression, were 90.5% and 90.3% for control MT-1 cells and HBZ-knockdown MT-1 cells, respectively. Suppressed HBZ expression led to increase the *Bim* gene transcription (Fig. 5J and K), indicating that HBZ expression is linked to suppression of *Bim* expression in ATL cells.

Discussion

Human immunodeficiency virus type 1 (HIV-1) replicates vigorously and the generated virus infects target cells *in vivo*. Unlike HIV-1, HTLV-1 induces proliferation to increase the number of infected cells, as this virus is transmitted primarily by cell-to-cell contact (5). Therefore, HTLV-1–encoded proteins promote proliferation of infected cells and inhibit their apoptosis, resulting in an increased number of infected cells *in vivo* (2). In this study, we show that HBZ inhibits both the intrinsic and extrinsic apoptotic pathways via targeting FoxO3a, which leads to suppressed transcriptions of *Bim* and *FasL*. We demonstrated two mechanisms for perturbation of FoxO3a by HBZ: interaction of HBZ with FoxO3a and interference of nuclear export of phosphorylated FoxO3a. HBZ suppresses DNA-binding ability of active form of FoxO3a through interaction between central domain of HBZ and forkhead domain of FoxO3a. In addition, LXXLL-like motif of HBZ is implicated in inhibition of FoxO3a-mediated apoptosis, suggesting that HBZ interferes in interaction of CBP/p300 and FoxO3a. Furthermore, HBZ retains inactive form of FoxO3a in the nucleus through interaction with 14-3-3, leading to transcriptional repression of the target genes. Interestingly, accumulation of phosphorylated form of FoxO3a in the nucleus has been observed in HIV Vpr-expressing cells, which might be implicated in HIV-mediated resistance against insulin (28). Thus, FoxO3a is a target of both human retroviruses.

In this study, we showed that central domain of HBZ interacts with FoxO3a while LXXLL-like motif in activation domain of HBZ is responsible for suppressed apoptosis. LXXLL-like motif of HBZ has been reported to interact with KIX domain of p300 (38). The central domain of HBZ interacts with the forkhead domain of FoxO3a, which binds to the target sequence (35). This is the mechanism how HBZ inhibits DNA binding of FoxO3a. However, inhibitory effect of HBZ on apoptosis largely depends on LXXLL-like motif of activation domain (Fig. 2A and B). FoxO3a is also reported to interact with KIX domain of CBP/p300 (37). Forkhead domain of FoxO3a intramolecularly interacts with its conserved regions (CR) 3, and binding of forkhead domain to DNA releases CR3, allowing it to bind KIX of CBP/p300 (45). These findings suggest that HBZ interferes in the complex interaction between FoxO3a and CBP/p300, which is likely important to induce apoptosis.

It has been reported that Bim has a tumor-suppressor function in various cancers. Hemizygous loss of the *Bim* gene promoted development of B-cell leukemia in Myc-transgenic mice in which c-myc expression was driven by the immunoglobulin gene intron-enhancer (46). Insulin-like growth factor 1 (IGF-1), an important growth factor for myeloma cells, has been reported to suppress Bim expression by epigenetic and posttranslational mechanisms (25). In Epstein–Barr virus–infected B cells, *Bim* transcription is silenced by DNA methylation of the *Bim* gene promoter (47). Thus, impaired expression of Bim is associated with the various cancers, including the virus-related malignancies. FoxO3a is also a target of oncogenesis. BCR-ABL induces phosphorylation of FoxO3a, which leads to suppressed expression of Bim in $Ph1^+$ chronic myelogenous leukemia cells (32). In breast cancer, IκB kinase interacts with, phosphorylates FoxO3a, which causes proteolysis of FoxO3a (48). In this study, we revealed that HBZ hinders nuclear export of phosphorylated FoxO3a, and impairs function of FoxO3a likely through interaction of FoxO3a and p300. Thus, suppressed Bim and FasL expression through inhibition of FoxO3a by HBZ is a new mechanism for oncogenesis.

Besides FoxO3a perturbation by HBZ, we also have identified the epigenetic aberrations in the promoter region of the *Bim* gene in ATL cells, and found that Bim expression is suppressed by DNA methylation and histone modification. ATL cell lines exhibited upregulated level of H3K27 trimethylation in the promoter regions of *Bim*. It has been reported that enhancer of zeste (EZH) 2, a methyltransferase and component of the polycomb repressive complex 2, expression is increased in ATL cell lines (42). Because EZH2 plays an essential role in the epigenetic maintenance of H3K27 trimethylation, upregulated H3K27 trimethylation of the *Bim* gene promoter might be associated with increased expression of EZH2 in ATL cells. In addition, HBZ seems to be associated with histone deacetylation in MT-1 cells. According to the previous studies, it is known that both HBZ and FoxO3a bind to the histone acetyltransferase p300/CBP through the LXXLL motif (38). In this study, we found that the same motif is important for FoxO3a suppression and resulting inhibition of apoptosis. It is likely that HBZ decreases histone acetylation level on Bim promoter through the interaction with FoxO3a and dissociation of p300/CBP from the promoter. In addition to histone modifications, hypermethylation of CpGs in Bim promoter was observed in some ATL cells. These epigenetic aberrations likely occur as the secondary changes following long-time silencing of *Bim* by HBZ, although further investigations will be required.

Published OnlineFirst October 31, 2013; DOI: 10.1158/0008-5472.CAN-13-0436

In this study, we demonstrated that HBZ suppresses activation-induced apoptosis by downregulation of proapoptotic genes, *Bim* and *FasL*. HBZ perturbs the function of FoxO3a by interaction, and induces epigenetic aberrations in the promoter region of the *Bim* gene. It has been shown that HBZ induces not only cancer but also inflammation *in vivo*. Because inflammatory diseases are essentially caused by failure to negatively regulate unnecessary immune responses by apoptosis, suppression of apoptosis by HBZ might be associated with HTLV-1–induced inflammation as well. Collectively, HBZ-mediated inhibition of apoptosis is likely implicated in both neoplastic and inflammatory diseases caused by HTLV-1.

Disclosure of Potential Conflicts of Interest

No potential conflicts of interest were disclosed.

Authors' Contributions

Conception and design: A. Tanaka-Nakanishi, J. Yasunaga, M. Matsuoka
Development of methodology: A. Tanaka-Nakanishi, M. Matsuoka
Acquisition of data (provided animals, acquired and managed patients, provided facilities, etc.): A. Tanaka-Nakanishi, K. Takai
Analysis and interpretation of data (e.g., statistical analysis, biostatistics, computational analysis): A. Tanaka-Nakanishi, J. Yasunaga, K. Takai, M. Matsuoka
Writing, review, and/or revision of the manuscript: A. Tanaka-Nakanishi, J. Yasunaga, M. Matsuoka
Administrative, technical, or material support (i.e., reporting or organizing data, constructing databases): M. Matsuoka
Study supervision: M. Matsuoka

Acknowledgments

The authors thank T. Furuyama (Kagawa Prefectural University of Health Science) for the 6xDBE-Luc plasmid DNA, P. Bouillet for valuable comments on this study, and L. Kingsbury for proofreading of this manuscript.

Grant Support

This study was supported by a Grant-in-aid for Scientific Research from the Ministry of Education, Science, Sports, and Culture of Japan to M. Matsuoka (MEXT grant number 221S0001), a grant from Japan Leukemia Research Fund to M. Matsuoka, and a grant from the Takeda Science Foundation to J. Yasunaga.

The costs of publication of this article were defrayed in part by the payment of page charges. This article must therefore be hereby marked *advertisement* in accordance with 18 U.S.C. Section 1734 solely to indicate this fact.

Received February 14, 2013; revised September 12, 2013; accepted October 5, 2013; published OnlineFirst October 31, 2013.

References

1. Proietti FA, Carneiro-Proietti AB, Catalan-Soares BC, Murphy EL. Global epidemiology of HTLV-I infection and associated diseases. Oncogene 2005;24:6058–68.
2. Matsuoka M, Jeang KT. Human T-cell leukaemia virus type 1 (HTLV-1) infectivity and cellular transformation. Nat Rev Cancer 2007;7:270–80.
3. Igakura T, Stinchcombe JC, Goon PK, Taylor GP, Weber JN, Griffiths GM, et al. Spread of HTLV-I between lymphocytes by virus-induced polarization of the cytoskeleton. Science 2003;299:1713–6.
4. Pais-Correia AM, Sachse M, Guadagnini S, Robbiati V, Lasserre R, Gessain A, et al. Biofilm-like extracellular viral assemblies mediate HTLV-1 cell-to-cell transmission at virological synapses. Nat Med 2010;16:83–9.
5. Derse D, Hill SA, Lloyd PA, Chung H, Morse BA. Examining human T-lymphotropic virus type 1 infection and replication by cell-free infection with recombinant virus vectors. J Virol 2001;75:8461–8.
6. Mazurov D, Ilinskaya A, Heidecker G, Lloyd P, Derse D. Quantitative comparison of HTLV-1 and HIV-1 cell-to-cell infection with new replication dependent vectors. PLoS Pathog 2010;6:e1000788.
7. Cavrois M, Leclercq I, Gout O, Gessain A, Wain-Hobson S, Wattel E. Persistent oligoclonal expansion of human T-cell leukemia virus type 1-infected circulating cells in patients with Tropical spastic paraparesis/HTLV-1 associated myelopathy. Oncogene 1998;17:77–82.
8. Etoh K, Tamiya S, Yamaguchi K, Okayama A, Tsubouchi H, Ideta T, et al. Persistent clonal proliferation of human T-lymphotropic virus type I-infected cells *in vivo*. Cancer Res 1997;57:4862–7.
9. Grassmann R, Aboud M, Jeang KT. Molecular mechanisms of cellular transformation by HTLV-1 Tax. Oncogene 2005;24:5976–85.
10. Fan J, Ma G, Nosaka K, Tanabe J, Satou Y, Koito A, et al. APOBEC3G generates nonsense mutations in HTLV-1 proviral genomes *in vivo*. J Virol 2010;84:7278–87.
11. Satou Y, Yasunaga J, Yoshida M, Matsuoka M. HTLV-I basic leucine zipper factor gene mRNA supports proliferation of adult T cell leukemia cells. Proc Natl Acad Sci U S A 2006;103:720–5.
12. Satou Y, Yasunaga J, Zhao T, Yoshida M, Miyazato P, Takai K, et al. HTLV-1 bZIP factor induces T-cell lymphoma and systemic inflammation *in vivo*. PLoS Pathog 2011;7:e1001274.
13. Bouillet P, O'Reilly LA. CD95, BIM and T cell homeostasis. Nat Rev Immunol 2009;9:514–9.
14. Debatin KM, Goldman CK, Waldmann TA, Krammer PH. APO-1-induced apoptosis of leukemia cells from patients with adult T-cell leukemia. Blood 1993;81:2972–7.
15. Yasunaga J, Taniguchi Y, Nosaka K, Yoshida M, Satou Y, Sakai T, et al. Identification of aberrantly methylated genes in association with adult T-cell leukemia. Cancer Res 2004;64:6002–9.
16. Krueger A, Fas SC, Giaisi M, Bleumink M, Merling A, Stumpf C, et al. HTLV-1 Tax protects against CD95-mediated apoptosis by induction of the cellular FLICE-inhibitory protein (c-FLIP). Blood 2006;107:3933–9.
17. Okamoto K, Fujisawa J, Reth M, Yonehara S. Human T-cell leukemia virus type-I oncoprotein Tax inhibits Fas-mediated apoptosis by inducing cellular FLIP through activation of NF-kappaB. Genes Cells 2006;11:177–91.
18. Sun SC, Yamaoka S. Activation of NF-kappaB by HTLV-I and implications for cell transformation. Oncogene 2005;24:5952–64.
19. Zhao T, Yasunaga J, Satou Y, Nakao M, Takahashi M, Fujii M, et al. Human T-cell leukemia virus type 1 bZIP factor selectively suppresses the classical pathway of NF-kappaB. Blood 2009;113:2755–64.
20. Brunet A, Bonni A, Zigmond MJ, Lin MZ, Juo P, Hu LS, et al. Akt promotes cell survival by phosphorylating and inhibiting a Forkhead transcription factor. Cell 1999;96:857–68.
21. Zhao T, Satou Y, Sugata K, Miyazato P, Green PL, Imamura T, et al. HTLV-1 bZIP factor enhances TGF-{beta} signaling through p300 coactivator. Blood 2011;118:1865–76.
22. Furuyama T, Nakazawa T, Nakano I, Mori N. Identification of the differential distribution patterns of mRNAs and consensus binding sequences for mouse DAF-16 homologues. Biochem J 2000;349:629–34.
23. Ponchel F, Toomes C, Bransfield K, Leong FT, Douglas SH, Field SL, et al. Real-time PCR based on SYBR-Green I fluorescence: an alternative to the TaqMan assay for a relative quantification of gene rearrangements, gene amplifications and micro gene deletions. BMC Biotechnol 2003;3:18.
24. Richter-Larrea JA, Robles EF, Fresquet V, Beltran E, Rullan AJ, Agirre X, et al. Reversion of epigenetically mediated BIM silencing overcomes chemoresistance in Burkitt lymphoma. Blood 2010;116:2531–42.
25. De Bruyne E, Bos TJ, Schuit F, Van Valckenborgh E, Menu E, Thorrez L, et al. IGF-1 suppresses Bim expression in multiple myeloma via epigenetic and posttranslational mechanisms. Blood 2010;115:2430–40.
26. Fan J, Kodama E, Koh Y, Nakao M, Matsuoka M. Halogenated thymidine analogues restore the expression of silenced genes without demethylation. Cancer Res 2005;65:6927–33.

Published OnlineFirst October 31, 2013; DOI: 10.1158/0008-5472.CAN-13-0436

27. Kumaki Y, Oda M, Okano M. QUMA: quantification tool for methylation analysis. Nucleic Acids Res 2008;36:W170–5.
28. Kino T, De Martino MU, Charmandari E, Ichijo T, Outas T, Chrousos GP. HIV-1 accessory protein Vpr inhibits the effect of insulin on the Foxo subfamily of forkhead transcription factors by interfering with their binding to 14-3-3 proteins: potential clinical implications regarding the insulin resistance of HIV-1-infected patients. Diabetes 2005;54:23–31.
29. Cante-Barrett K, Gallo EM, Winslow MM, Crabtree GR. Thymocyte negative selection is mediated by protein kinase C- and Ca2+-dependent transcriptional induction of bim [corrected]. J Immunol 2006;176:2299–306.
30. Snow AL, Oliveira JB, Zheng L, Dale JK, Fleisher TA, Lenardo MJ. Critical role for BIM in T cell receptor restimulation-induced death. Biol Direct 2008;3:34.
31. Green DR, Droin N, Pinkoski M. Activation-induced cell death in T cells. Immunol Rev 2003;193:70–81.
32. Essafi A, Fernandez de Mattos S, Hassen YA, Soeiro I, Mufti GJ, Thomas NS, et al. Direct transcriptional regulation of Bim by FoxO3a mediates STI571-induced apoptosis in Bcr-Abl-expressing cells. Oncogene 2005;24:2317–29.
33. Busuttil V, Droin N, McCormick L, Bernassola F, Candi E, Melino G, et al. NF-kappaB inhibits T-cell activation-induced, p73-dependent cell death by induction of MDM2. Proc Natl Acad Sci U S A 2010;107:18061–6.
34. Brunet A, Park J, Tran H, Hu LS, Hemmings BA, Greenberg ME. Protein kinase SGK mediates survival signals by phosphorylating the forkhead transcription factor FKHRL1 (FOXO3a). Mol Cell Biol 2001;21:952–65.
35. Obsil T, Obsilova V. Structure/function relationships underlying regulation of FOXO transcription factors. Oncogene 2008;27:2263–75.
36. Modur V, Nagarajan R, Evers BM, Milbrandt J. FOXO proteins regulate tumor necrosis factor-related apoptosis inducing ligand expression. Implications for PTEN mutation in prostate cancer. J Biol Chem 2002;277:47928–37.
37. Wang F, Marshall CB, Yamamoto K, Li GY, Gasmi-Seabrook GM, Okada H, et al. Structures of KIX domain of CBP in complex with two FOXO3a transactivation domains reveal promiscuity and plasticity in coactivator recruitment. Proc Natl Acad Sci U S A 2012;109:6078–83.
38. Clerc I, Polakowski N, Andre-Arpin C, Cook P, Barbeau B, Mesnard JM, et al. An interaction between the human T cell leukemia virus type 1 basic leucine zipper factor (HBZ) and the KIX domain of p300/CBP contributes to the down-regulation of tax-dependent viral transcription by HBZ. J Biol Chem 2008;283:23903–13.
39. Tsai KL, Sun YJ, Huang CY, Yang JY, Hung MC, Hsiao CD. Crystal structure of the human FOXO3a-DBD/DNA complex suggests the effects of post-translational modification. Nucleic Acids Res 2007;35:6984–94.
40. Bouillet P, Zhang LC, Huang DC, Webb GC, Bottema CD, Shore P, et al. Gene structure alternative splicing, and chromosomal localization of pro-apoptotic Bcl-2 relative Bim. Mamm Genome 2001;12:163–8.
41. Gilley J, Ham J. Evidence for increased complexity in the regulation of Bim expression in sympathetic neurons: involvement of novel transcriptional and translational mechanisms. DNA Cell Biol 2005;24:563–73.
42. Gilley J, Coffer PJ, Ham J. FOXO transcription factors directly activate bim gene expression and promote apoptosis in sympathetic neurons. J Cell Biol 2003;162:613–22.
43. Marks P, Rifkind RA, Richon VM, Breslow R, Miller T, Kelly WK. Histone deacetylases and cancer: causes and therapies. Nat Rev Cancer 2001;1:194–202.
44. Fullgrabe J, Kavanagh E, Joseph B. Histone onco-modifications. Oncogene 2011;30:3391–403.
45. Wang F, Marshall CB, Li GY, Yamamoto K, Mak TW, Ikura M. Synergistic interplay between promoter recognition and CBP/p300 coactivator recruitment by FOXO3a. ACS Chem Biol 2009;4:1017–27.
46. Egle A, Harris AW, Bouillet P, Cory S. Bim is a suppressor of Myc-induced mouse B cell leukemia. Proc Natl Acad Sci U S A 2004;101:6164–9.
47. Paschos K, Smith P, Anderton E, Middeldorp JM, White RE, Allday MJ. Epstein-barr virus latency in B cells leads to epigenetic repression and CpG methylation of the tumour suppressor gene Bim. PLoS Pathog 2009;5:e1000492.
48. Hu MC, Lee DF, Xia W, Golfman LS, Ou-Yang F, Yang JY, et al. IkappaB kinase promotes tumorigenesis through inhibition of forkhead FOXO3a. Cell 2004;117:225–37.

別紙４

研究成果の刊行に関する一覧表

研究代表者　京都大学ウイルス研究所　　教授　　松岡雅雄
研究分担者　九州大学大学院歯学研究院　教授　　中村誠司

書籍

著者氏名	論文タイトル名	書籍全体の編集者名	書　籍　名	出版社名	出版地	出版年	ページ
森山雅文、**中村誠司**	「シェーグレン症候群：最新の知見」、シェーグレン症候群の発症と病態進展におけるTh サブセットの関与	宮坂信之	炎症と免疫	先端医学社	東京	2013	111-118

雑誌

発表者氏名	論文タイトル名	発表誌名	巻号	ページ	出版年
Tsuboi H, Hagiwara S, Asashima H, Umehara H, Kawakami A, Nakamura H, Sano H, Tsubota K, Ogawa Y, Takamura E, Saito I, Inoue H, **Nakamura S**, (他7名)	Validation of different sets of criteria for the diagnosis of Sjögren's syndrome in Japanese patients	Mod Rheumatol.	23(2)	219-25	2013
Tsuboi H, Asashima H, Takai C, Hagiwara S, Yokosawa M, Hirota T, Umehara H, Kawakami A, Nakamura H, Sano H, Tsubota K, Ogawa Y, Takamura E, Saito I, Inoue H, **Nakamura S**, (他8名)	Primary and secondary surveys on epidemiology of Sjögren's syndrome in Japan	Mod Rheumatol.		In press	2013
Moriyama M, Tanaka A, Maehara T, Furukawa S, Nakashima H, **Nakamura S**	T helper subsets in Sjögren's syndrome and IgG4-related dacryoadenitis and sialoadenitis: A critical review.	J Autoimmun		In press	2013

Mod Rheumatol (2013) 23:219–225
DOI 10.1007/s10165-012-0812-9

ORIGINAL ARTICLE

Validation of different sets of criteria for the diagnosis of Sjögren's syndrome in Japanese patients

Hiroto Tsuboi · Shinya Hagiwara · Hiromitsu Asashima · Hisanori Umehara · Atsushi Kawakami · Hideki Nakamura · Hajime Sano · Kazuo Tsubota · Yoko Ogawa · Etsuko Takamura · Ichiro Saito · Hiroko Inoue · Seiji Nakamura · Masafumi Moriyama · Tsutomu Takeuchi · Yoshiya Tanaka · Shintaro Hirata · Tsuneyo Mimori · Isao Matsumoto · Takayuki Sumida

Received: 8 November 2012 / Accepted: 5 December 2012 / Published online: 28 December 2012

Abstract
Objective To validate the revised Japanese Ministry of Health criteria for the diagnosis of Sjögren's syndrome (SS) (JPN) (1999), The American-European Consensus Group classification criteria for SS (AECG) (2002), and American College of Rheumatology classification criteria for SS (ACR) (2012).
Methods The study subjects were 694 patients with SS or suspected SS who were followed-up in June 2012 at ten hospitals that form part of the Research Team for Autoimmune Diseases, The Research Program for Intractable Disease by the Ministry of Health, Labor and Welfare (MHLW). All patients had been checked for all four criteria of the JPN (pathology, oral, ocular, anti-SS-A/SS-B antibodies). We studied the clinical diagnosis made by the physician in charge and the satisfaction of the above criteria.
Results Of the 694 patients, 499 patients did not have other connective tissue diseases (CTDs). SS was diagnosed in 476 patients (primary SS in 302, secondary SS in 174), whereas non-SS was diagnosed in 218 patients (without other CTDs in 197, with other CTDs in 21) by the physician in charge. The sensitivities of JPN, AECG, and ACR in the diagnosis of all forms of SS (both primary and secondary SS) were 79.6, 78.6, and 77.5 %, respectively, with respective specificities of 90.4, 90.4, and 83.5 %. The sensitivities of the same systems in the diagnosis of primary SS were 82.1, 83.1, and 79.1 %, respectively, with specificities of 90.9, 90.9, and 84.8 %, respectively. The sensitivities of the same systems in the diagnosis of secondary SS were 75.3, 70.7, and 74.7 %, respectively, with specificities of 85.7, 85.7, and 71.4 %, respectively.
Conclusion The sensitivity of JPN to all forms of SS and secondary SS, the sensitivity of AECG to primary SS, and the specificities of JPN and AECG for all forms of SS, primary SS, and secondary SS were highest in the diagnosis of SS in Japanese patients. These results indicate that

H. Tsuboi · S. Hagiwara · H. Asashima · I. Matsumoto · T. Sumida (✉)
Department of Internal Medicine, Faculty of Medicine, University of Tsukuba, 1-1-1 Tennodai, Tsukuba, Ibaraki 305-8575, Japan
e-mail: tsumida@md.tsukuba.ac.jp

H. Tsuboi · H. Umehara · A. Kawakami · H. Nakamura · H. Sano · K. Tsubota · Y. Ogawa · E. Takamura · I. Saito · H. Inoue · S. Nakamura · M. Moriyama · T. Takeuchi · Y. Tanaka · S. Hirata · T. Mimori · T. Sumida
The Research Team for Autoimmune Diseases, The Research Program for Intractable Disease of the Ministry of Health, Labor and Welfare (MHLW), Tokyo, Japan

H. Umehara
Department of Hematology and Immunology, Kanazawa Medical University, Kanazawa, Japan

A. Kawakami · H. Nakamura
Unit of Translational Medicine, Department of Immunology and Rheumatology, Nagasaki University Graduate School of Biomedical Sciences, Nagasaki, Japan

H. Sano
Division of Rheumatology, Department of Internal Medicine, Hyogo College of Medicine, Nishinomiya, Japan

K. Tsubota · Y. Ogawa
Department of Ophthalmology, School of Medicine, Keio University, Tokyo, Japan

E. Takamura
Department of Ophthalmology, Tokyo Women's Medical University, School of Medicine, Tokyo, Japan

the JPN criteria for the diagnosis of SS in Japanese patients are superior to ACR and AECG.

Keywords Sjögren's syndrome · Criteria

Introduction

Sjögren's syndrome (SS) is an autoimmune disease that affects exocrine glands, including the salivary and lacrimal glands. It is characterized by lymphocytic infiltration into the exocrine glands, leading to dry mouth and eyes. A number of autoantibodies, such as anti-SS-A and SS-B antibodies, are detected in patients with SS. SS is subcategorized into primary SS, which is not associated with other well-defined connective tissue diseases (CTDs), and secondary SS, which is associated with other well-defined CTDs [1]. Primary SS is further subcategorized into the glandular form and the extraglandular form.

The revised criteria for the diagnosis of SS issued by the Japanese Ministry of Health (JPN) (1999) (Table 1) [2], as well as the American-European Consensus Group classification criteria for SS (AECG) (2002) (Tables 2, 3) [1], are usually used in both daily clinical practice and clinical studies in Japan. Thus, two sets of diagnostic systems are being applied for the same disease. This could result in a heterogeneous pool of SS patients. This heterogeneity of SS patients makes it difficult to analyze the diagnosis, efficacy of treatment, and prognosis of SS patients. A better alternative would be to use a unified set of criteria for the diagnosis of SS in Japan. Recently, The American College of Rheumatology (ACR) published the ACR classification criteria for SS (2012) (Table 4), which were proposed by the Sjögren's International Collaborative Clinical Alliance (SICCA) [3]. The new set of criteria is designed to be used worldwide, not only in advanced countries but also in developing countries. The SICCA established a uniform classification for SS based on a combination of objective tests that have known specificity to SS [3].

Table 1 The revised Japanese Ministry of Health criteria for the diagnosis of SS (1999)

1. Histopathology
Definition: Positive for at least one of (A) or (B)
(A) Focus score ≥1 (periductal lymphoid cell infiltration ≥50) in a 4 mm^2 minor salivary gland biopsy
(B) Focus score ≥1 (periductal lymphoid cell infiltration ≥50) in a 4 mm^2 lacrimal gland biopsy
2. Oral examination
Definition: Positive for at least one of (A) or (B)
(A) Abnormal findings in sialography ≥stage 1 (diffuse punctate shadows of <1 mm)
(B) Decreased salivary secretion (flow rate ≤10 ml/10 min according to the chewing gum test or ≤2 g/2 min according to the Saxon test) and decreased salivary function according to salivary gland scintigraphy
3. Ocular examination
Definition: Positive for at least one of (A) or (B)
(A) Schirmer's test ≤5 mm/5 min and rose bengal test ≥3 according to the van Bijsterveld score
(B) Schirmer's test ≤5 mm/5 min and positive fluorescein staining test
4. Serological examination
Definition: Positive for at least one of (A) or (B)
(A) Anti-Ro/SS-A antibody
(B) Anti-La/SS-B antibody
Diagnostic criteria: diagnosis of SS can be made when the patient meets at least two of the above four criteria

Upon comparing these three classification sets, there are some differences among them in their purpose and the items adopted in the set (Table 5). The JPN criteria (1999) are intended as an aid for diagnosis, whereas the AECG criteria (2002) and the ACR criteria (2012) are intended for classification purposes in clinical studies and trials. Although the ACR criteria include only three objective items (Tables 4, 5) and are the simplest among the three sets, the ACR criteria may not identify SS patients with negative findings in labial salivary gland biopsy, because the ACR criteria do not include salivary secretion analysis and imaging studies. On the other hand, the JPN criteria combined oral examinations such as salivary secretion, sialography, and salivary gland scintigraphy with three objective items adopted in the ACR criteria (Table 5). Only the AECG criteria include ocular and oral symptoms, which may cause false positives in patients with non-SS conditions such as aging or visual display terminals (VDT) syndrome (Table 5).

I. Saito · H. Inoue
Department of Pathology, Tsurumi University School of Dental Medicine, Yokohama, Kanagawa, Japan

S. Nakamura · M. Moriyama
Section of Oral and Maxillofacial Oncology, Division of Maxillofacial Diagnostic and Surgical Sciences, Faculty of Dental Science, Kyushu University, Fukuoka, Japan

T. Takeuchi
Division of Rheumatology, Department of Internal Medicine, School of Medicine, Keio University, Tokyo, Japan

Y. Tanaka · S. Hirata
The First Department of Internal Medicine, School of Medicine, University of Occupational and Environmental Health, Kitakyushu, Japan

T. Mimori
Department of Rheumatology and Clinical Immunology, Kyoto University Graduate School of Medicine, Kyoto, Japan

Table 2 The American-European Consensus Group classification criteria for SS (2002)

I. Ocular symptoms: a positive response to at least one of the following questions
1. Have you had daily, persistent, troublesome dry eyes for more than 3 months?
2. Do you have a recurrent sensation of sand or gravel in the eyes?
3. Do you use tear substitutes more than 3 times a day?
II. Oral symptoms: a positive response to at least one of the following questions
1. Have you had a daily feeling of dry mouth for than 3 months?
2. Have you had recurrently or persistently swollen salivary glands as an adult?
3. Do you frequently drink liquids to aid in swallowing dry food?
III. Ocular signs—that is, objective evidence of ocular involvement defined as a positive result for at least one of the following two tests
1. Schirmer's test, performed without anaesthesia ($\leq$5 mm in 5 min)
2. Rose bengal score or other ocular dry eye score ($\geq$4 according to van Bijsterveld's scoring system)
IV. Histopathology: in minor salivary glands (obtained through normal-appearing mucosa) focal lymphocytic sialoadenitis, evaluated by an expert histopathologist, with a focus score $\geq$1, defined as a number of lymphocytic foci (which are adjacent to normal-appearing mucous acuni and contain more than 50 lymphocytes) per 4 mm^2 of glandular tissue
V. Salivary gland involvement: objective evidence of salivary gland involvement defined by a positive result for at least one of the following diagnostic tests
1. Unstimulated whole salivary flow ($\leq$1.5 ml in 15 min)
2. Parotid sialography showing the presence of diffuse sialectasias (punctate, cavitary or destructive pattern), without evidence of obstruction in the major ducts
3. Salivary scintigraphy showing delayed uptake, reduced concentration and/or delayed excretion of tracer
VI. Autoantibodies: presence in the serum of the following autoantibodies
1. Antibodies to Ro (SS-A) or La (SS-B) antigens, or both

Table 3 The American-European Consensus Group classification criteria for SS (2002) rules for classification

For primary SS
In patients without any potentially associated disease, primary SS may be defined as follows:
(A) The presence of any 4 of the 6 items is indicative of primary SS, as long as either item IV (histopathology) or VI (serology) is positive
(B) The presence of any 3 of the 4 objective criteria items (that is, items III, IV, V, VI)
For secondary SS
In patients with a potentially associated disease (for instance, another well-defined connective tissue disease), the presence of item I or item II plus any 2 from among items III, IV, and V may be considered as indicative of secondary SS
Exclusion criteria:
Past head and neck radiation treatment
Hepatitis C infection
Acquired immunodeficiency disease (AIDS)
Pre-existing lymphoma
Sarcoidosis
Graft vs. host disease
Use of anticholinergic drugs (for a time shorter than 4-fold the half life of the drug)

The purpose of the present study was to validate the JPN criteria, AECG criteria, and ACR criteria for the diagnosis of SS in Japanese patients. The study identified the differences among these three classification sets.

Patients and methods

Study population

The study subjects were 694 patients (51 males and 643 females) with a diagnosis of SS or suspected SS who had been checked for all four criteria of the JPN (pathology, oral, ocular, anti-SS-A/SS-B antibody), and were followed up in June 2012 at ten hospitals across Japan (Kanazawa Medical University Hospital, Nagasaki University Hospital, Hyogo Medical University Hospital, Keio University Hospital, Tokyo Women's Medical University Hospital, Tsurumi University Hospital, Kyushu University Hospital, University of Occupational and Environmental Health Hospital, Kyoto University Hospital, and University of Tsukuba Hospital) that form part of the Research Team for Autoimmune Diseases, The Research Program for Intractable Disease of the Ministry of Health, Labor and Welfare (MHLW).

Data collection and analysis

We collected clinical data from the above ten hospitals using a questionnaire. We retrospectively examined the clinical diagnosis made by the physician in charge, as well as the satisfaction of the JPN, AECG, and ACR criteria. Because lissamine green ocular staining had not been adopted in Japan at the time of clinical examination, we regarded patients who had a positive rose bengal test or fluorescein staining test as having satisfied the ocular staining score in the ACR classification system.

We regarded the clinical diagnosis made by the physician in charge as the gold standard for the diagnosis of SS in this study. We compared the sensitivities and specificities of the JPN, AECG, and ACR diagnostic systems in the diagnosis of SS (both primary and secondary SS), primary

Table 4 The American College of Rheumatology classification criteria for SS (2012)

The classification of SS, which applies to individuals with signs/symptoms that may be suggestive of SS, will be met in patients who have at least 2 of the following 3 objective features:
1. Positive serum anti-SS-A/Ro and/or anti-SS-B/La or (positive rheumatoid factor and ANA titer ≥1:320)
2. Labial salivary gland biopsy exhibiting focal lymphocytic sialadenitis with a focus score ≥1 focus/4 mm^2
3. Keratoconjunctivitis sicca with ocular staining score ≥3 (assuming that individual is not currently using daily eye drops for glaucoma and has not had corneal surgery or cosmetic eyelid surgery in the last 5 years)
Prior diagnosis of any of the following conditions would exclude participation in SS studies or therapeutic trials because of overlapping clinical features or interference with criteria tests:
History of head and neck radiation treatment
Hepatitis C infection
Acquired immunodeficiency syndrome
Sarcoidosis
Amyloidosis
Graft vs. host disease
IgG4-related disease

SS, and secondary SS. Agreement between the three was assessed via the kappa coefficient.

Results

Diagnosis of SS (primary and secondary SS) and non-SS

Of the 694 patients, 499 patients did not have other well-defined CTDs, whereas 195 patients did. SS was diagnosed in 476 patients (302 primary SS, 174 secondary SS), whereas non-SS was diagnosed in 218 patients (197 without other CTDs, 21 with other CTDs) by the physician in charge (Table 6).

Sensitivities and specificities of the three diagnostic systems for SS

The sensitivities of JPN, AECG, and ACR in the diagnosis of all SS (302 primary SS and 174 secondary SS) were 79.6, 78.6, and 77.5 %, respectively, whereas the respective specificities in the diagnosis of all SS were 90.4, 90.4, and 83.5 %. The sensitivities of JPN, AECG, and ACR in the diagnosis of 302 primary SS were 82.1, 83.1, and 79.1 %, respectively, with specificities of 90.9, 90.9, and 84.8 %, respectively. The sensitivities of JPN, AECG, and ACR in the diagnosis of 174 secondary SS were 75.3, 70.7, and 74.7 %, respectively, with specificities of 85.7, 85.7, and 71.4 % (Table 7).

Table 5 Comparison of the items adopted in the JPN and AECG and ACR criteria

	JPN	AECG	ACR
Ocular symptoms	×	○	×
Oral symptoms	×	○	×
Ocular signs			
Schirmer's test	○	○	×
Ocular staining	○	○	○
Labial salivary gland biopsy	○	○	○
Salivary gland involvements			
Salivary secretion	○	○	×
Sialography	○	○	×
Scintigraphy	○	○	×
Autoantibodies			
SS-A	○	○	○
SS-B	○	○	○
ANA	×	×	○
RF	×	×	○

SS-A anti-SS-A antibody, *SS-B* anti-SS-B antibody, *ANA* anti-nuclear antibody, *RF* rheumatoid factor, ○ adopted, × not adopted, *JPN* the revised Japanese Ministry of Health criteria for the diagnosis of Sjögren's syndrome (1999), *AECG* The American-European Consensus Group classification criteria for Sjögren's syndrome (2002), *ACR* American College of Rheumatology classification criteria for Sjögren's syndrome (2012)

Table 6 Diagnosis of SS and non-SS

	Associated with other CTDs		Total
	No	Yes	
Clinical diagnosis			
SS	302 (primary SS)	174 (secondary SS)	476
Non-SS	197	21	218
Total	499	195	694

Clinical diagnosis diagnosis of SS by the physician in charge
CTDs connective tissue diseases

Comparisons of the satisfaction of the three diagnostic systems

Figure 1 displays Venn diagrams showing comparisons of the satisfaction of the three diagnostic systems. Among all SS patients ($n = 476$), more patients satisfied only the AECG criteria ($n = 42$) rather than only the JPN criteria ($n = 8$) or the ACR criteria ($n = 6$). The same tendency was also observed in patients with primary SS only and in those with secondary SS only. The diagrams indicate that the JPN and ACR diagnostic systems are similar, whereas the AECG diagnostic system is different from the other two. Table 8 shows the agreement among the three

Table 7 Sensitivities and specificities of the three tested systems for diagnosing SS

	Entire group		Without other CTDs		With other CTDs	
	Sensitivity	Specificity	Sensitivity	Specificity	Sensitivity	Specificity
JPN	79.6	90.4	82.1	90.9	75.3	85.7
AECG	78.6	90.4	83.1	90.9	70.7	85.7
ACR	77.5	83.5	79.1	84.8	74.7	71.4

The "entire group" comprised 694 patients, including 476 with SS (302 patients with primary SS and 174 with secondary SS) and 218 patients with non-SS. The "without other CTDs" group of 499 patients included 302 patients with primary SS and 197 with non-SS. The "with other CTDs" group of 195 patients included 174 patients with secondary SS and 21 with non-SS

JPN Japanese Ministry of Health criteria for the diagnosis of Sjögren's syndrome (1999), *AECG* The American-European Consensus Group classification criteria for Sjögren's syndrome (2002), *ACR* The American College of Rheumatology classification criteria for Sjögren's syndrome (2012)

diagnostic systems, as assessed using the kappa coefficient. The data indicate a high level of agreement between the JPN and ACR diagnostic systems (kappa coefficient 0.74), but a low level of agreement between AECG and the other two (kappa coefficient 0.10–0.46) in the diagnosis of all SS, primary SS, and secondary SS.

Discussion

While it is difficult to select the best gold standard system for the diagnosis of CTDs such as systemic lupus erythematosus (SLE), rheumatoid arthritis (RA), and SS, this issue is clinically relevant and important. In SLE, the ACR revised criteria for the classification of SLE (1997) [4] has been adopted for diagnosis in daily clinical practice and for classification purposes in clinical studies. Recently, the Systemic Lupus International Collaborating Clinics (SLICC) has proposed new classification criteria for SLE [5], which has generated interesting discussion about these two criteria among expert rheumatologists. On the other hand, for RA, the 2010 RA classification criteria: an ACR/European League Against Rheumatism (EULAR) collaborative initiative [6] was published recently and is currently used not only in clinical studies for the classification of RA but also in daily clinical practice for the diagnosis of RA. Therefore, these available diagnostic systems for SLE and RA could be regarded as the gold standard for both clinical studies and daily clinical practice. The AECG criteria have been adopted in Western countries for the diagnosis of SS. In Japan, however, both the AECG and JPN criteria are currently being used simultaneously for the classification and diagnosis of SS. On the other hand, the new ACR criteria have been proposed as a uniform classification for SS. At present, there is no gold standard system for the diagnosis of SS in both clinical studies and daily clinical practice, except for expert judgment. This state could create a heterogeneous pool of SS patients, which makes it difficult to analyze the diagnosis, efficacy of treatment, and prognosis of SS patients. Establishing a single set of criteria for SS and selecting a gold standard system for the diagnosis of SS is an important task in Japan.

The present study demonstrated that the sensitivity of the JPN system for all SS and secondary SS, the sensitivity of the AECG system for primary SS, and the specificities of the JPN and AECG systems for all SS, primary SS, and secondary SS were highest among the three systems for diagnosing SS in Japanese patients (relative to clinical judgment as the gold standard). The results also showed high agreement between the JPN and ACR systems, but low agreement between AECG and the other two diagnostic systems for all SS, primary SS, and secondary SS. These results indicate that the JPN and ACR criteria covered similar patient populations, although the sensitivity and specificity were higher for the JPN system than the ACR system. Among the 302 patients with primary SS, 14 did not satisfy the ACR criteria for the diagnosis of SS, although they did meet the criteria of both JPN and AECG. Further analysis of these 14 SS patients also showed that 50 % of these patients had negative pathological findings, 70 % had negative ocular staining, and 50 % were negative for autoantibodies (data not shown). These SS patients could be misdiagnosed by the ACR criteria, resulting in the lower sensitivity of the ACR diagnostic system. On the other hand, among 197 non-SS patients without other CTDs, ten patients satisfied the ACR criteria but not the JPN nor the AECG criteria (data not shown). Further analysis of these ten patients indicated that 80 % were positive for lissamine green ocular staining (Schirmer's test, rose bengal staining, and fluorescein staining were not performed), and 60 % were positive for anti-SS-A antibody (data not shown). Although these patients might be misdiagnosed as primary SS by the ACR criteria, this could not be confirmed because these patients could be positive for other ocular tests adopted by the JPN and AECG diagnostic systems.

The specificities of the criteria for all SS, primary SS, and secondary SS patients used in the JPN and AECG

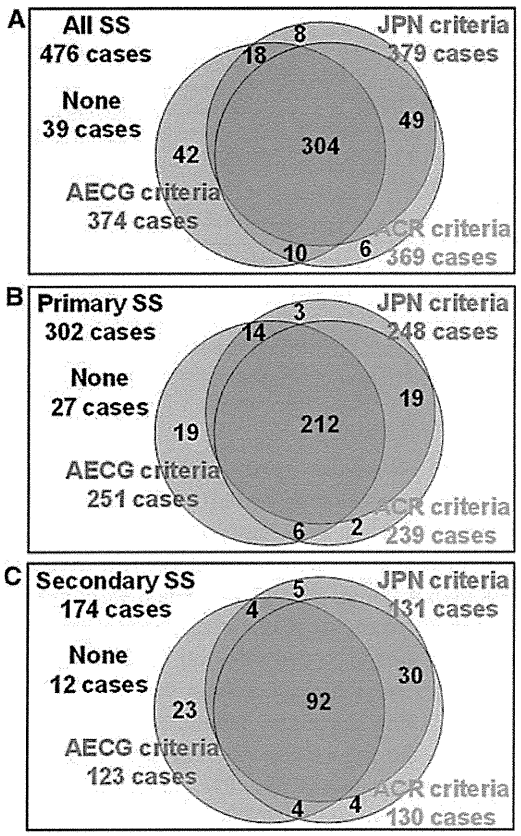

Fig. 1 Venn diagrams showing a comparison of the satisfaction of the three tested systems. **a** Comparison of the satisfaction of the three tested systems, performed using data from all 476 SS patients (302 primary SS and 174 secondary SS). **b** Comparison of the satisfaction of the three tested systems using data on 302 patients with primary SS. **c** Comparison of the satisfaction of the three tested systems using data on 174 patients with secondary SS. *Numbers* show the numbers of patients who satisfied each set of criteria, *None* indicates the number of patients who did not satisfy the criteria of any of the three systems. *JPN criteria* the revised Japanese Ministry of Health criteria for the diagnosis of SS (1999), *AECG criteria* The American-European Consensus Group classification criteria for SS (2002), *ACR criteria* American College of Rheumatology classification criteria for SS (2012)

systems were the same in this study. The reason for the same specificities of the JPN and AECG criteria may be the identical number of non-SS patients (21 patients, including 18 patients without CTDs and 3 patients with CTDs) who satisfied JPN and AECG. However, the JPN and AECG profiles for 20 out of these 21 non-SS patients were completely different, highlighting the low agreement between JPN and AECG, as shown in Table 8.

The sensitivity of AECG for primary SS was highest among the three systems, whereas that of JPN for all SS and secondary SS was highest. Among the 302 primary SS patients, 19 patients only satisfied the AECG criteria. These 19 primary SS patients had high frequencies of dry eye (84.2 %) and dry mouth (100.0 %) but low frequencies of anti-SS-A antibody (10.5 %) and anti-SS-B antibody (0 %). These seronegative primary SS patients with symptoms of dryness could only be diagnosed by the AECG criteria, because only the AECG criteria include symptoms of dryness. This may be the sensitivity of AECG for primary SS was highest among the three systems.

The above findings suggest that JPN provided the best set of criteria necessary for the diagnosis of Japanese patients with SS. Admittedly, however, the results of the present study do not allow us to confirm the superiority of JPN due to the inherent limitations of the study. First, we used the clinical judgment of the physician in charge as the gold standard. In Japan, because the JPN criteria are the criteria used most commonly in daily clinical practice, the clinical judgment could depend on the satisfaction of the JPN criteria. It is better to rely on expert committee consensus based on clinical case scenarios as the gold standard for diagnosis in order to avoid this bias. Second, patients who had been checked for all four criteria of the JPN diagnostic system (pathology, oral, ocular, anti-SS-A/SS-B antibodies) were included in this study, but the methods used for ocular staining varied among the participating institutions. Third, the results of the study could include selection bias. For these reasons, we need a more

Table 8 Agreement among the three tested systems, as assessed using the kappa coefficient

All SS ($n = 476$)	All SS ($n = 476$) (primary SS, $n = 302$, secondary SS, $n = 174$)	Primary SS ($n = 302$)	Secondary SS ($n = 174$)
JPN vs. AECG	0.31	0.46	0.10
JPN vs. ACR	0.74	0.74	0.74
AECG vs. ACR	0.30	0.42	0.12

The "entire group" comprised 694 patients, including 476 with SS (302 patients with primary SS and 174 with secondary SS) and 218 patients with non-SS. The "without other CTDs" group of 499 patients included 302 patients with primary SS and 197 with non-SS. The "with other CTDs" group of 195 patients included 174 patients with secondary SS and 21 with non-SS.

JPN Japanese Ministry of Health criteria for the diagnosis of Sjögren's syndrome (1999), *AECG* The American-European Consensus Group classification criteria for Sjögren's syndrome (2002), *ACR* The American College of Rheumatology classification criteria for Sjögren's syndrome (2012)